FE Simulation of High Frequency Mechanical Impact (HFMI) Treatment – First Results

Stefanos Gkatzogiannis*,[a], Peter Knoedel[a], Thomas Ummenhofer[a]

[a]Karlsruhe Insittute of Technology, KIT Steel & Lightweight Structures
stefanos.gkatzogiannis@kit.edu
peter knoedel@kit.edu
thomas.ummenhofer@kit.edu

ABSTRACT

High Frequency Mechanical Impact treatment is investigated numerically in the present paper. A first-step numerical dynamic analysis is carried out using the solver LS-Dyna. The treatment of an unnotched component of S355 is simulated. The strain rate dependent material parameter Cowper-Symonds is calibrated for the investigated material based on data from literature. Goal of the present analysis is to act a first step for a robust engineering approach, which will calculate with sufficient preciseness the residual stresses introduced by this post-weld treatment. The calculated residual stresses of the present investigation are compared with respective measurements found in literature. Deviation between measured and simulated residual stresses indicates the need for further improvement of the present model.

Keywords: HFMI, fatigue, weld treatment, residual stresses

1   LIST OF SYMBOLS

t	[s]	time
m	[kg]	mass
c	[(N x s)/m]	damping
u	[m]	displacement
Fs(u)	[N]	resisting force as a function of deformation
p(t)	[N]	external transient loading
f_o	[Hz]	initial frequency
ξ	[-]	damping coefficient
σ_y and σ_y'	[Pa]	static and dynamic yield strength
C and q	[-]	coefficients of the Cowper-Symonds model with no direct physical meaning
$\dot{\varepsilon}_{pl}$	[s⁻¹]	equivalent plastic strain rate
F_r	[N]	friction force
μ	[-]	friction coefficient

2   INTRODUCTION

In the last decades, several methods have been developed for increasing fatigue life of welds. High Frequency Mechanical Impact treatment (HFMI) (1) is one of the most straightforward and effective (see (2)). The method is based on the acceleration of a pin made of hardened steel towards the weld toe by an appropriate mechanism. Each HFMI-device manufacturer applies a different mechanism for accelerating the pin, but the mechanical effect on the weldment remains the same. Compressive

residual stresses (RS), which counterbalance the tensile welding residual stresses (WRS), are introduced, the notch effect is reduced and the treated surface becomes locally hardened. A significant increase of fatigue strength of even more than 100 % in some cases is possible due to these changes (see (1)). The effectiveness of HFMI for the extension of fatigue life has been thoroughly validated though experimental investigations in the past (see (2), (3), (4) etc.). The effectiveness of the method has been confirmed for various geometries, plate thicknesses and nominal strengths of parent material. Still, the HFMI enhancement of fatigue strength depends on many parameters (5).

FE simulation of HFMI could act alternatively and/or supplementary to the cost ineffective fatigue tests. It could enable a safe prediction of the introduced RS field in practice, taking into consideration the various unique parameters of each investigated case, such as welding residual stresses, notch effect, complex geometries, material properties etc.. FE simulation of welding has evolved rapidly in the last decades and calculation of WRS through engineering approaches is possible with sufficient preciseness (6). HFMI has been as well studied numerically in several studies during the last years (see (2), (7), (8), (9), (10), etc.). Nevertheless, in many cases significant discrepancies, like insufficient modelling of material behaviour, movement of the HFMI pin and boundary conditions, have been observed.

The present study is a first step for the documentation of a fully validated numerical investigation of HFMI taking into consideration all the significant aspects. The treatment of an unnotched component is simulated, as a first step validation of the present engineering approach, based on material data and validated with RS measurements found in literature. A first overview regarding the influence of several factors of the simulation on the simulated RS is enabled through the present study.

3 THEORETICAL BACKGROUND

3.1 Analysis type

A significant deformation rate of the treated metal is observed during HFMI treatment. It has been reported that strain rates between 200 s^{-1} and 400 s^{-1} are met (9). Neglection of dynamic effects could lead to erroneous results and a full dynamic analysis has to be carried out for the simulation of HFMI. The dynamic analysis, taking into consideration non-linear material behaviour is governed by the following equation of motion (*Eq. (1)*).

$$m \cdot \ddot{u} + c \cdot \dot{u} + F_S(u) = p(t) \tag{1}$$

Therefore, precise modelling of damping and material constitutive law are perquisites for a precise simulation of the investigated process. Viscous damping models like the one presented in *Eq. (2)* have been widely applied in recent simulations of shot peening by Kim et al. (11), (13), a process of similar principle to HFMI, especially from a modelling point of view.

$$c = 2 \cdot f_0 \cdot \xi \cdot m \tag{2}$$

Different values for ξ were tested by Kim et al. and the value of 0.5 was proposed for ξ due to numerical efficiency reasons. The same damping model with the same damping factor ξ = 0.5 was applied as well by Yuan et al. during numerical analysis of HFMI in (10). No other consideration of damping in previous analyses of HFMI is known to the authors of the present study.

3.2 Modelling Material Behaviour

With regard to modelling of material behaviour, yield strength is predominant for the present analysis. The significance of yield strength during FE simulation of HFMI was highlighted by Le Quilliec et al. in (7). Nonetheless, for strain rates like the above-mentioned, which clearly deviate from the static case ($\dot{\varepsilon} \rightarrow 0\ s^{-1}$), yield strength of steel is dependent on strain rate. This dependency was proven non-negligible even in weld simulations, where much lower strain rates were met (0.122 s^{-1}), as it was shown in a previous investigation of the authors (13).

Moreover, when multiple impacts along a line take place, areas of the component that were subjected to compressive straining could be now deforming under tension and vice versa. Kinematic hardening, taking into consideration the Bauschinger effect would be expected to provide better results, as it describes better the plastic behaviour of steels under reversed plasticity at room temperature.

Moreover, according to (15) the effect can be even more profound under high strain rates in some cases. On the other hand, according to common knowledge, validity of the Bauschinger effect is restricted to a region of plastic strains, smaller than those present during HFMI treatment. The influence of hardening behaviour was investigated by Hardenacke et al. (8). Isotropic, combined and rate-dependent hardening models produced qualitatively similar results in depth direction, but as in the case of the WRS, significant deviation to the magnitude of the peak RS was met. In other previous simulations of HFMI, Zheng et al. (15), Le Quillec et al. (7) and Baptista (20) applied combined, isotropic and kinematic and Chaboche hardening models respectively, while Yuan et al. used usual linear kinematic hardening (10). The suitability of kinematic and Chaboche-based mixed hardening models was compared by Foehrenbach et al. in (9). The applied Chaboche model was found to provide better results near the treatment surface. The Cowper-Symonds material model, which is presented in *Eq. (4)* enables the incorporation of the Bauschinger effect with kinematic or mixed material models and allows for consideration of the strain rate dependency.

$$\dot{\varepsilon}_{pl} = C \cdot \left(\frac{\sigma_{y'}}{\sigma_y} - 1 \right)^q \tag{4}$$

3.3 Modelling of the HFMI Pin
HFMI pin is manufactured of hardened high strength steel. Negligible linear elastic deformation of the pin is expected. In comparison to the significant plastic strains that are introduced to the treated component, deformation of the pin could possibly be considered negligible without undermining the preciseness of the results. In previous studies of HFMI the pin was simulated as elastic (20), (7), (10), or rigid (4), (9), (8), (15). The analogous simulation of shot peening by Kim et al. comparing results from analyses with rigid elastic and plastic spheres concluded that the later one provides better results (11). Yet during shot peening, deformation of the shots is observed in reality as well, which is not the case for HFMI.

Nonetheless, modelling the pin's movement is expected to be more predominant, as the respective kinetic energy is transformed to strain energy introducing the plastic deformation and in extension the RS to the treated component. Two different approaches for modelling the movement of the pin can be applied: A displacement-based, forcing the pin to move to a predefined trace (4), (7), (15), (17) and a force-based, applying appropriate accelerating force to the pin in order to achieve a specific impact velocity (10), (20). It is easily understood that the former one is much more straightforward as a measurement of the HFMI trace is much easier than the documentation of the impact speed. On the other hand, the latter method is much closer to physical reality. The two approaches were compared in (8) and (9) and it was concluded that displacement-based analysis provides results with sufficient preciseness.

3.4 Modelling the Contact Conditions
The friction between the pin and the treated surface has to be taken into consideration as well, as it leads to consumption of the kinetic energy of the pin. A Coulomb friction model was proposed in (4) for simulating the friction between metallic parts. The model is described by *Eq. (4)*

$$F_r = \mu \cdot N \tag{4}$$

4 INVESTIGATED COMPONENT

The unnotched component of Fig. 1a with dimensions 20 mm x 20 mm x 10 mm made of S355 was investigated in the present study. A symmetry plane was applied and it is presented as well in Fig. 1. A treatment length of 5 mm, beginning at 2 mm from the edge of the component, was selected in the present study. A treatment velocity and frequency of 24 cm/min and 90 Hz respectively were assumed for the present component and HFMI method. The real component investigated by Foehrenbach et al. (9) had a length of 30 mm and a longer treatment line. This deviation would serve a dual role in the present study: decrease the computational time for a preliminary analysis like the present one and allow the investigation of the scaling effect. The latter one was of great interest, as according to an assumption of the authors, the localized nature of the RS from the HFMI treatment, would allow the

investigation of large-scale components on models of smaller scale. Each treatment pass begun 0.1 mm away from the previous along the treatment line, so that the impacts of each pass would not completely overlap with those of the prior treatment.

A full transient analysis for a displacement-based solution is carried out with the commercial FE software LS DYNA (18). Meshing and pre-processing of the model was carried out in commercial FE software ANSYS Workbench (19). An element size of 0.1 mm was applied for meshing the treated area and the pin in all directions, while larger elements of 1 mm were applied away from them. The applied mesh is presented in Fig. 1b. 3 treatment passes were carried out on the real component and respective traces of 0.173 mm, 0.1796 mm and 0.241 mm were measured after each pass. The same vertical displacement was applied for the movement of the pin, neglecting at this first step the elastic strain spring back after the end of the treatment. Values of the friction coefficient for mild steel found in (19) are applied for the present simulation.

Cowper-Symonds material model was applied for the present simulation using nominal yield strength and tangent modulus value of 2.2 GPa for S355 found in (6). Parameters C and q were set, equal to 18250 and 5 respectively. A kinematic hardening material behaviour was selected. Displacement of the nodes on the bottom of the component was fixed in all directions (u_x, u_y, u_z). An impedance boundary allowing complete flow of stress waves was applied on side of the component opposite to the symmetry plane, simulating in this way a semi-infinite solid. It was considered that the width of the real component was large enough for this assumption. Moreover, it was intended to investigate the above-mentioned scaling effect with regard to length of the component and treatment line and exclude width from this consideration.
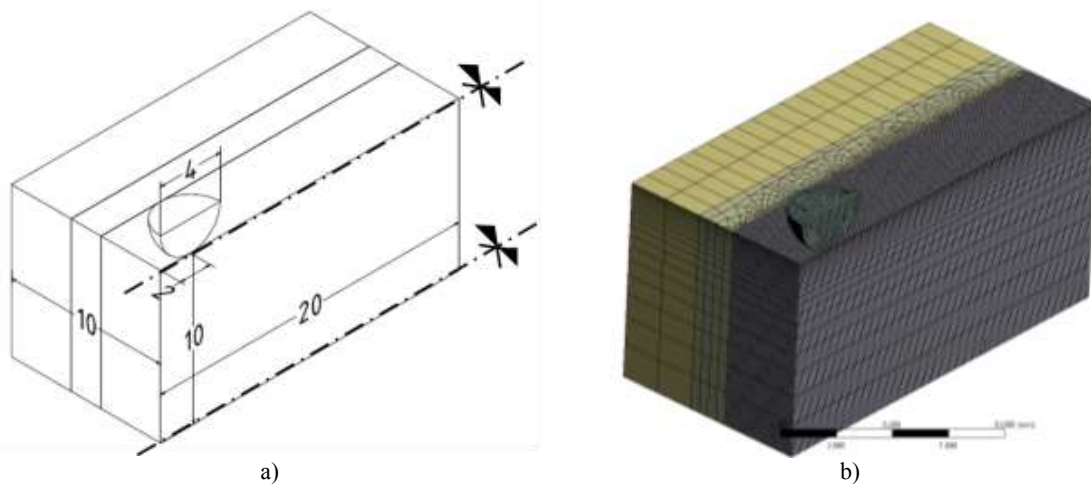

Fig. 1. a) Investigated component, dimensions are given in mm; b) The applied mesh

5   RESULTS AND DISCUSSION

The simulated and measured RS after each treatment pass are presented in Fig. 2. The calculated RS profiles in all cases seem to follow qualitatively the pattern of the measurements from larger depths up to a point between 1 mm and 2 mm away from the surface. Significant discrepancies, even qualitatively, are met at the surface and down to a depth of 2 mm for the results regarding the 1st pass of the treatment. The difference lies up to 200 MPa for the longitudinal RS and even higher for the transverse. This deviation seems to be gradually reduced for the longitudinal RS as the treatment passes increase. After the 3rd treatment, no deviation larger than 100 MPa is observed for the longitudinal RS. Improvement is met as well for the transverse RS although on a smaller scale. At higher depths, the agreement of measured and simulated longitudinal RS is sufficient in all cases.

The effect of improved preciseness with the higher number of simulated treatment passes is expected, due to the increased step along treatment line that is considered during consecutive impacts in the present analysis. The real step, which is roughly estimated to be ten times smaller, allows for

significant overlapping of consecutive impacts at the real component. Therefore, one real treatment pass corresponds to multiple passes in the simulation. Nevertheless, a significantly smaller step of the pin cannot be modelled due to numerical reasons. However, more analyses should be carried out in order to clarify if the increased step is the reason for the present discrepancies.
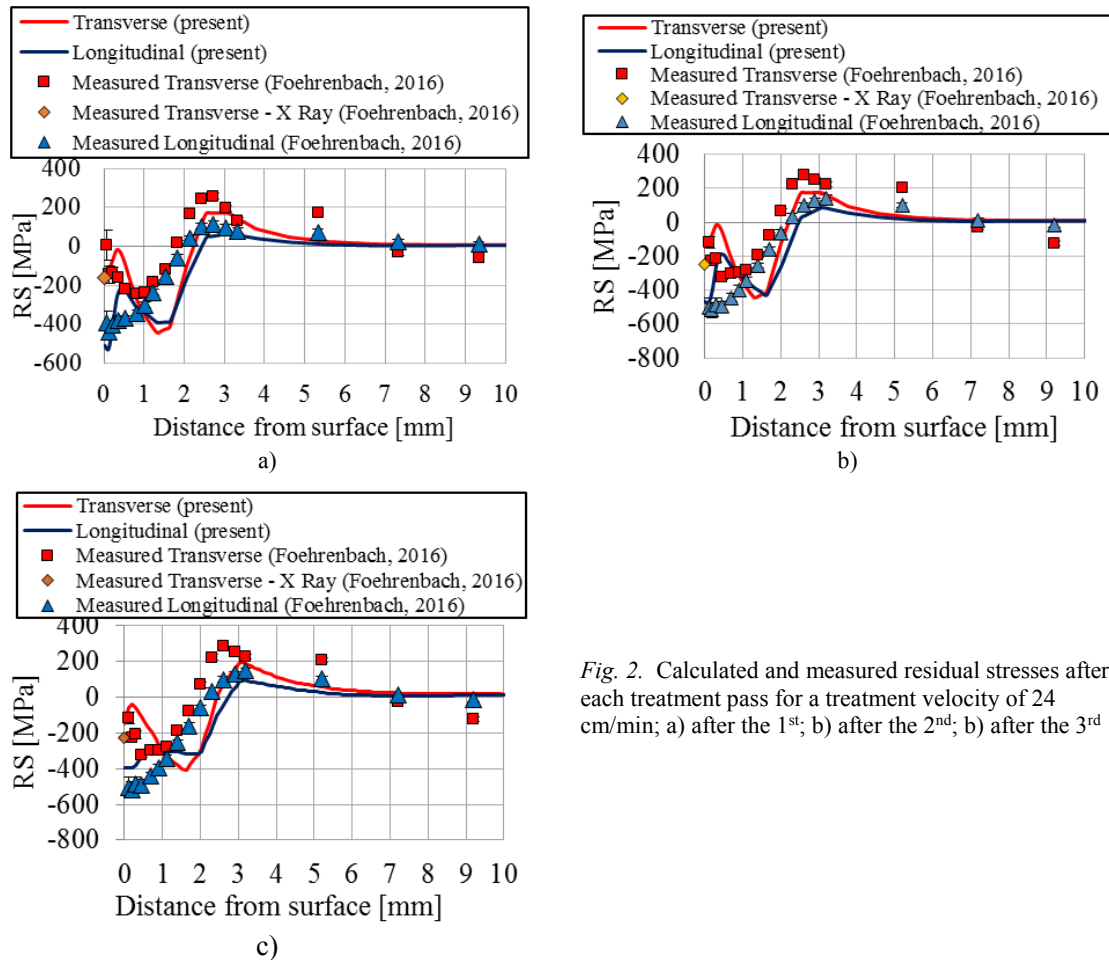

a)

b)

c)

Fig. 2. Calculated and measured residual stresses after each treatment pass for a treatment velocity of 24 cm/min; a) after the 1st; b) after the 2nd; b) after the 3rd

6   CONCLUSIONS AND FUTURE WORK

The present results are considered insufficient due to the significant deviation between calculated and measured RS. Improvement of the results must be achieved, before conclusions regarding the aspects of the HFMI modelling can be drawn. The increased simulated step of the pin, the use of nominal yield strength and kinematic hardening and the neglection of elastic spring back of the deformed component during simulation of pin's displacement, can be accounted for the deviation between measurements and simulation. These issues will be resolved, so that better agreement is met.

7   ACKNOWLEDGEMENT

The present study was carried out in the framework of the first author's doctoral dissertation (21).

REFERENCES

1. **Marquis, G. B. and Barsoum, Z.** *IIW Recommendations for the HFMI Treatment – For Improving the Fatigue Strength of Welded Joints.* Singapore : Springer Singapore (IIW Collection), 2016.
2. **Ummenhofer, T., et al.** *REFRESH: Lebensdauerverlängerung bestehender und neuer geschweißter Stahlkonstruktionen, Abschlussbericht D 761.* Karlsruhe : KIT Stahl- und Leichtbau, Versuchsanstalt für Stahl, Holz und Steine, 2009.

3. **Ummenhofer, T., Weich, I. and Nitschke-Pagel, T.** Lebens- und Restlebensdauerverlängerung geschweißter Windenergieanlagentürme und anderer Stahlkonstruktionen durch Schweißnahtnachbehandlung. *Stahlbau.* 2005, Vol. 74, 6, pp. 412-422.

4. **Ummenhofer, T., et al.** *Erhöhung der Ermüdungsfestigkeit von Offshore-Windenergieanlagen durch Schweißnahtnachbehandlung unter Berücksichtigung des Korrosionseinflusses, Research project, DVS 09069 – IGF 18457 N.* s.l. : Karlsruhe. KIT Stahl- und Leichtbau, Versuchsanstalt für Stahl, Holz und Steine. München. Hochschule für angewandte Wissenschaften , Labor für Stahl- und Leichtmetallbau, 2018.

5. **Ummenhofer, T. and Weidner, P.** Improvement Factors for the Design of Welded Joints subjected to High Frequency Mechanical Impact Treatment. *Steel Construction.* 2013, Vol. 6, 3, pp. 191-199.

6. **Knoedel, P., Gkatzogiannis, S. and Ummenhofer, T.** Practical Aspects of Welding Residual Stress Simulation. *Journal of Constructional Steel Research .* 2017, Vol. 132, pp. 83-96.

7. **Le Quilliec, G., et al.** Fatigue Behaviour of Welded Joints Treated by High Frequency Hammer Peening: Part II, Numerical Study. *IIW Commission XIII, Doc. XIII -2395-11.* 2011.

8. **Hardenacke, V., et al.** Modelling and Simulation of the High Frequency Mechanical Impact (HFMI) Treatment of Welded Joints. *IIW Commission XIII, Doc. XIII-2533-14,.* 2014.

9. **Foehrenbach, J., Hardenacke, V. and Farajian, M.** High Frequency Mechanical Impact Treatment (HFMI) for the Fatigue Improvement: Numerical and Experimental Investigations to describe the Condition in the Surface Layer. *Welding in the World.* 2016, Vol. 60, 4, pp. 749-755.

10. **Yuan, K. L. and Sumi, Y.** Modelling of Ultrasonic Impact Treatment (UIT) of Welded Joints and its Effect on Fatigue Strength. *Frattura ed Integrità Strutturale.* 2015, Vol. 34, pp. 476–486,.

11. **Kim, T., et al.** A Simple but Effective FE Model with Plastic Shot for Evaluation of Peening Residual Stress And its Experimental Validation. *Science and Engineering A.* 2011, Vol. 528, pp. 5945–5954.

12. **Kim, T., et al.** A 3D FE Model with Plastic Shot for Evaluation of Equi-Biaxial Peening Residual Stress due to Multi-Impacts. *Surface & Coatings Technology.* 2012, Vol. 206, pp. 3125–3136.

13. **Gkatzogiannis S., Knoedel P., Ummenhofer T.** Strain Rate Dependency of Simulated Welding Residual Stresses. *Journal of Material Performance and Engineering.* 2017, Vol. 27, 10, pp. 5079-5085.

14. **Peirs, J., Verleysen, P. and Degrieck, J.** Study of the Dynamic Bauschinger Effect in Ti6Al4V by Torsion Experiments. *EPJ web of Conferences.* 2012, Vol. 26.

15. **Zheng, J., Ince, A. and Tang, L.** *Modelling and Simulation of Weld Residual Stresses and Ultrasonic Impact Treatment of Welded Joints.* Senlis : 7th International Conference of Fatigue Design, 29-30 November, 2017.

16. **Baptista, R., Infante, V. and Branco, C.** Fully Dynamic Numerical Simulation of the Hammer Peening Fatigue Life Improvement Technique. *Procedia Engineering.* 2011, Vol. 10, pp. 1943-1948.

17. **Mangering, I., Kroyer, R. and Koller, M.** Experimental and Numerical Analysis of the Effectiveness of High-Frequency Peening Processes. *Steel Construction.* 2017, Vol. 10, 1, pp. 54-66.

18. **LS-DYNA.** *Theory Manual.* US : Livermore Software Technology Corporation (LSTC), 2016.

19. **ANSYS®.** *Academic Research, Release 19.2, Help System.* US : ANSYS, Inc., 2018.

20. **Avallone, E. A. and Baumeister, T. I.** *Marks' Standard Handbook for Mechanical Engineers.* New York : McGraw-Hill, 10th Edition, 1996.

21. **Gkatzogiannis, S.** *Finite Element Simulation of Residual Stresses from Welding and High Frequency Hammer Peening.* Doctoral Dissertation : Kalrsruhe Institute of Technology, Steel- and Lightweight Structures, to be submitted in 2019.